

Predictive Biomarkers of Brain tumor Lesions through Correlation of Histopathological changes with Metabolites by Magnetic Resonance Spectroscopy

H. Smitha^{1*}, V.N. Meena Devi², K.S. Sreekanth³, J. Vinoo⁴

¹Department of Physics, Noorul Islam Centre of Higher Education, Kumarakovil, Kanyakumari & Department of Physiology, Sree Gokulam Medical College & Research Foundation, Venjaramoodu.P.O. Trivandrum, India

²Department of Physics, Noorul Islam Centre of Higher Education, Kumarakovil, Kanyakumari, India

³Department of Biochemistry, Sree Gokulam Medical College & Research Foundation, enjaramoodu.P.O.Trivandrum, India

⁴Department of Radio Diagnosis, Sree Gokulam Medical College & Research Foundation, Venjaramoodu.P.O.Trivandrum, India

► Original article

ABSTRACT

*Corresponding author:

Haridas Smitha,

E-mail:

smithavinod2000@yahoo.co.in

Received: February 2022

Final revised: April 2023

Accepted: May 2023

Int. J. Radiat. Res., October 2023;
21(4): 769-777

DOI: 10.52547/ijrr.21.4.24

Keywords: brain tumors, magnetic resonance spectroscopy, metabolites

Background: Brain tumors like intracranial metastases, meningioma, gliomas, etc are the most prevalent brain tumors. Magnetic Resonance Spectroscopy (MRS) helps in the differentiation of high grade, low grade brain tumors, brain neoplasms, etc. **Materials and Methods:** This study was conducted in the Radiology Department of one of the major tertiary health care centers in South Kerala. Patients suspected of brain tumors were subjected to both MRS and histopathological examinations after the surgery. A total of 69 patients were included. Histopathological findings were evaluated and grouped as benign, atypical, and anaplastic tumors and correlated with MRS findings. Statistical analysis was done by SPSS version 16. Friedman test was used for comparison. **Results:** In this study, MRS images of 69 brain tumor lesions were studied and compared for metabolic ratios and pathogenesis. MRS spectrum gives different peaks of specific metabolites of brain tumors like lipid, alanine, lactate, glycine, glutamate /glutamine, myoinositol, etc. Histopathological results also show different pathological findings. **Conclusions:** Magnetic Resonance Spectroscopy has a wide range of sensitivity to and is evaluate the different metabolites of brain lesions. The quantification of tissue metabolites can potentially identify the pathological change, at the biochemical level which creates further therapeutic interventions.

INTRODUCTION

As brain tumors are common, for their diagnosis and management there is a need for a basic understanding of diseases. Among all forms of cancers, brain tumors are the most feared type and also their survival rate is poor ^(1, 2). The abnormal growth of the tissue in the brain leads to harming the function of the brain, and it is associated with the progressive worsening of emotional and mental status ⁽³⁾. Any abnormal proliferation of cells, which may be either benign or malignant, is defined as a tumor ⁽⁴⁾. Brain tumors can be classified according to the cell of origin or the site of origin like neuronal-glia tumors, pineal tumors, embryonal tumors, tumors of cranial nerves, tumors of the meninges, lymphomas, hematopoietic neoplasms, germ cell tumors, tumors of the sellar region and metastases ⁽⁵⁾.

According to the fundamental research in the field of the pathogenesis of cancer, held at the cellular, molecular, and genetic levels of the organism, it was found that cancer is a process of

transformation of a normal cell into a tumor cell ⁽⁶⁾. During the progression of brain tumors, tumor-derived biomarkers like proteins, nucleic acids, and tumor-derived extracellular vesicles accumulate in the blood or cerebrospinal fluid. These circulating biomarkers play an important role in causing cancer ⁽⁷⁾. Due to some altered metabolic features, tumor cells rapidly produce fatty acids for membrane biosynthesis, lipidation reactions, and cellular signaling ⁽⁸⁾.

The histopathological evaluation as well as molecular diagnostics is helpful in therapeutic decision-making ⁽⁹⁾. The diagnosis of a brain tumor is dependent on appropriate brain imaging, especially gadolinium-enhanced magnetic resonance imaging ⁽¹⁰⁾. MRS (Magnetic Resonance Spectroscopy) provides a "molecular window" of a tissue into the component chemistry allowing an insight into the pathophysiologic process. MRS acts as a "molecular signature" of high grade and low grade tumors and can predict the aggressiveness of a tumor ⁽¹¹⁾. The metabolic alterations in different central nervous system pathologies can be determined by MRS as it is

used as a neuroradiological tool ⁽¹²⁾.

The development of Magnetic Resonance Imaging (MRI) like Magnetic Resonance Spectroscopy (MRS), provides non-anatomic information like neuronal density, cell-wall proliferation or degradation, and energy metabolism, in addition to anatomical information on body fluids, cell extracts, and tissue samples ^(13, 14). MRS gives the information to determine the concentration of brain metabolites such as N-acetyl aspartate (NAA), Choline (Cho), Creatine (Cr), and lactate in the tissue ⁽¹³⁾. By comparing the relative concentration of these metabolites, the information regarding neuronal cell density, cell membrane turnover, and possible necrosis can find out thereby the underlying pathology can be detected through MRS ⁽¹⁴⁾. MRS helps in the differentiation of high grade from low grade brain tumors, and also provides a neuroimaging biomarker of normal biological and pathological processes ^(15, 16). Cellular energy metabolism may alter during the tumor development and oncogene tumor/ suppressor gene pathways are the signalling pathways that are linked to the development of several tumors ⁽¹⁷⁾. Hence this study aims to find out the changes in metabolites in brain tumors diagnosed through MRS with the histopathological changes to predict specific biomarkers for brain tumor lesions.

MATERIALS AND METHODS

The study was conducted at the Department of Radiodiagnosis, Sree Gokulam Medical College & Research Foundation (SGMC & RF). The study was conducted as per the rules of the ethics committee for using the patients for scientific purposes after obtaining approval from the Institutional Ethics Committee (IEC) (registration number: SGMC-IEC N0 31/383/11/2018 (F) and date of registration: 26:11:2018).

Participants

In this study, 69 patients suspected of brain tumors were included. Patients were subjected to both MRS and histopathological examinations after surgery. Informed consent was taken from all the patients. Those with implants, aneurysm clips, pacemakers, heart valves, those who are not willing to participate in the study, and patients with ages below 20 years were excluded from this study.

MRS procedures

Among the 69 patients included in the study, there were patients with adenoma (n=6), cerebellopontine angle tumor (n=9), glioblastoma (n=6), glioma (n=4), lymphoma (n=6), meningioma (n=19), metastasis (n=8), oligodendroglioma (n=4), subependymoma (n=4) and tuberculoma (n=3). In this study Siemens - MAGNETOM ESSENZA 1.5 T MRI Scanner was used.

Also, the patients underwent MRS using a 1.5T MRI scanner. Only patients with proven MRS diagnosis for brain lesions were included as study subjects. Both males and females were included in the study.

All images were obtained by using spin-echo pulse sequences, gradient echo sequences, FLAIR and a two-dimensional Fourier transform image reconstruction. From all patients, we obtained T1-wt spin-echo images (Acquisition parameters -500-600/20-30/2-4 repetition time/echo time/excitations) and T2-wt spin-echo, FLAIR, gradient echo (2500-3000/30, 80/1). The images were acquired on a 256 x 256 matrix, with a field of view of 23 cm. All images had a slice thickness of 5mm and the number of slices taken was 20.

Initially, MRI scans were performed using 1.5 T. The MR imaging technique may be varied according to the indication of the examination. Usually, diffusion-weighted imaging techniques were included and perfusion-weighted MRI techniques have been performed routinely in cases of suspected tumors. Patients suspected of brain tumors are subjected to MRS examination. Both Single-voxel (SV) technique and the multivoxel technique were used. SV technique can be done by using long TR (Time of Repetition) and short TE (Time of Echo) and multivoxel technique using long TE. SV technique could demonstrate metabolites like myoinositol and lipids. The multivoxel technique could be used to demonstrate a larger area and could analyse the extent and heterogeneity of the pathologic area. The MR spectroscopic imaging data were acquired after the MR imaging was performed. During each examination, the heights and areas of the resonance peaks corresponding to Cho at 3.2 ppm, Cr at 3.0 ppm, and NAA at 2.0 ppm, were quantified. Based on the spectroscopic results of brain tumors, the concentrations of specific metabolites of each tumor were diagnosed and quantified to determine specific tumors, in addition to common metabolites observed in tumors like N-acetyl aspartate (NAA), creatine (Cr), and choline (Cho).

Histopathological procedures

The 69 patients with brain tumor lesions, who underwent surgical excision and confirmed on histopathology were prospectively studied in detail using H&E (Haematoxylin-Eosin-Saffron) staining. The patients suffering from adenoma (n=6), cerebellopontine angle tumor (n=9), glioblastoma (n=6), glioma (n=4), lymphoma (n=6), meningioma (n=19), metastasis (n=8), oligodendroglioma (n=4), subependymoma (n=4) and tuberculoma (n=3). The parameters studied were clinical features, histopathological features, and the WHO grade of the tumors. Histopathological evaluation and clinical information were assessed by using Routine Haematoxylin and Eosin. The Haematoxylin and Eosin stained paraffin sections and WHO

classifications of 2000 and 2007 were applied. The Haematoxylin and Eosin (H & E) stained slides of the cases were reviewed keeping in view the histological features. For the prospective study, biopsy tissue was fixed overnight in 10% buffered formalin and submitted for processing. Paraffin sections were cut 4 to 6 microns in thickness and routine H&E staining was performed. Special stains were performed. The results were analysed and data prepared to study histological patterns of brain tumors were evaluated according to the WHO classification of tumors of the central nervous system. Moreover, further studies are carried out to find out metabolic pathways thereafter the end products of the histopathological findings and correlated with MRS findings.

Statistical analysis

Statistical Analysis was performed by using SPSS version 16 software. The quantitative variables were expressed in mean and standard deviation (SD). Friedman Test was used for comparing the metabolic ratios. The statistical significance value was accepted as $p < 0.05$ in a 95% confidence interval.

RESULTS

In this study, MRS images of 69 brain tumor lesions were studied and compared for the metabolic ratios and extent of pathogenesis. The present study includes brain tumors (n=69) like adenoma, cerebellopontine angle tumor, glioblastoma, glioma, lymphoma, meningioma, metastasis, oligodendroglioma, subependymoma, tuberculoma. The results show that among the different groups of tumors, there is a deviation from normal values of common metabolites like N-acetyl aspartate (NAA), creatine (Cr), and choline (Cho). In addition to that, concentrations of specific metabolites like lipid, lactate, alanine, etc. for each tumor were also diagnosed.

Metabolic findings of brain tumors

The results show that, by analysing, one of the MRS spectra of adenoma (n=5) (figure A) gives peaks like lactate and lipids (1.32). It was also detected that there was an increased peak of Cho, and a reduced peak of NAA and Cr were observed. The tumor adenoma also shows that there was a significant difference as the p-value is 0.007. In figure B shows one of the spectra of cerebellopontine, which indicates the presence of lipid and lactate peak (an average value of 1.31). However, a reduced peak of Cr, NAA, and a dominant peak of Cho were also observed. It was observed that cerebellopontine shows, there was a significant difference as $p = 0.002$. Similarly, figure C, demonstrates one of the MRS spectra of glioblastoma (n=6) with an increase of lipids and also lactate, moreover, a reduced peak of

NAA and Cr, as well as an increased peak of Cho, were also detected. However, there was a statistically significant difference in glioblastoma ($p = 0.030$). Figure D shows one of the MRS spectra of glioma (n=4) that gives a lactate peak (an average value of 1.31). The lactate peaks were observed as inverted peaks. An increased level of myoinositol was also found in gliomas. An increased peak of Cho and a decreased peak of Cr and NAA were also observed. It was found that there were statistical differences were also observed in glioma ($p = 0.018$). By analysing, one of the MRS spectra of lymphoma (figure E) (n=6), an average value of prominent lipid peak at 1.3 was observed along with a decreased peak of NAA and Cr, but Cho levels were found to be increased. It was found that there was a statistically significant difference, in the lymphoma invented as $p = 0.02$. Figure F indicates the MRS spectrum of meningioma. It was found that one of the MRS of meningioma (n=19) gives the presence of lipids (1.43) in different concentrations. Alanine (average value, 1.34) was also present in the MRS spectrum of meningioma. In addition to that, it indicates it is a tumor, as it shows a decreased peak of NAA, Cr, and an increased peak of Cho. However, the meningioma gives a statistically significant difference as $p = .0001$. In figure G, the MRS spectrum of metastases (n=8) was characterized by a dominant peak of lipids at 1.3 ppm. In some case multiplets of the glutamine/glutamate complex was observed. The spectrum also shows that the NAA and Cr as reduced, and Cho has an elevated peak. It was detected that there were significant differences in metastasis were $p = 0.0001$. The spectrum of oligodendroglioma (figure H) (n=3) gives an increased level of lactate (an average value of 1.31) and myoinositol, an average value of 3.59, in addition to an increased Cho, decreased NAA, and decreased Cr peak. But it was found that there were no significant differences observed in oligodendroglioma ($p = 0.05$). In the case of subependymoma, one of the MRS (figure I) (n=7), the MRS shows the myoinositol (MI) (3.56) and glycine (Gly) peak. Moreover, an elevated peak of Cho and a declined peak of NAA and Cr were also noticed. In addition to that there was also a significant difference determined in the tumor, subependymoma as $p = 0.0001$. Figure J, depicts one of the MRS of tuberculoma (n=3), it shows that there were abnormally increased lipids, Glx, an average value of 1.38, 2.23 respectively, and also decreased peak of NAA, Cr, and an elevated peak of Cho. But the results show that there was no significant difference in the tumor tuberculoma $p = 0.050$.

Histopathological findings of brain tumors

Table 1, shows the histopathological analysis of adenoma, cerebellopontine angle tumor, glioblastoma, glioma, lymphoma, meningioma, metastasis, oligodendroglioma, subependymoma and tuberculoma. Typical histopathological

photomicrographs of brain tissues are shown on figures K to T. In the figure, histopathologic photomicrographs of brain tissues are given as K as an adenoma, L as a cerebellopontine angle tumor, M as a glioblastoma. And also N as Glioma; O as Meningioma; P as Lymphoma; Q-Metastatis; R-oligodendroglioma; S-subependymoma; T-tuberculoma (figure K).

The histopathological analysis of adenomas were detected as granulated GH-producing cells with large atypical ganglion cells in the pathological analysis. The histopathological report was given as circumscribed, encapsulated, biphasic, degenerative changes, nuclear pleomorphism, xanthomatous change, and vascular hyalinization, in the case of the cerebellopontine lesion. But glioblastoma was found as hypercellularity, nuclear atypical, microvascular proliferation, and necrosis. In addition to that the histopathological analysis, in the case of glioma were

also observed as hypercellularity, nuclear atypia and mitotic figures, and necrosis.

The histopathological analysis of lymphoma gives diffuse large B-cell lymphomas. But the meningiomas appeared as lobules, "meningothelial" whorls in the pathological analysis. In the case of metastasis the pathological report was observed as demarcated, spherical masses and shiny mucoid. On the other hand, oligodendroglioma appeared as round to oval, water-clear cytoplasm ringing along with lobulated nuclei. Moreover, the histopathological analyses were shown mitotic activity, microcalcifications, cystic degeneration, nuclear pleomorphism, vascular sclerosis, and hemosiderin deposition, in subependymoma, whereas the tuberculoma, shows clusters of small nodules. Table 2 shows the comparison of MRS findings and histopathological findings and the end products of metabolic pathways.

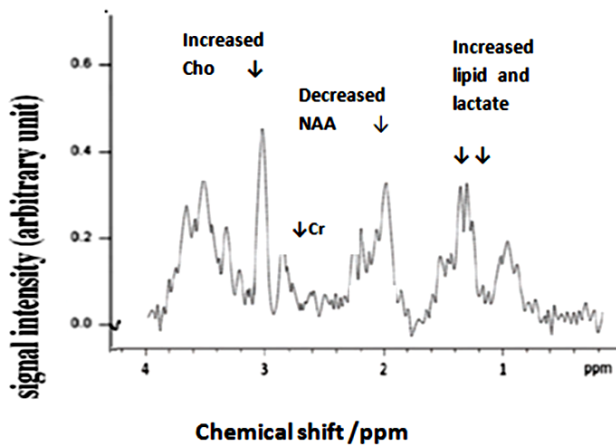


Figure A. The MR spectroscopy of Adenoma .The graph indicates signal intensity on the y-axis and chemical shift (ppm) on the x-axis. The spectroscopy reveals an elevated choline (Cho), a decreased peak of N-Acetyl Aspartate (NAA). The increased peaks of lipid (Lip) and lactate (Lac) give the characteristic feature of an adenoma.

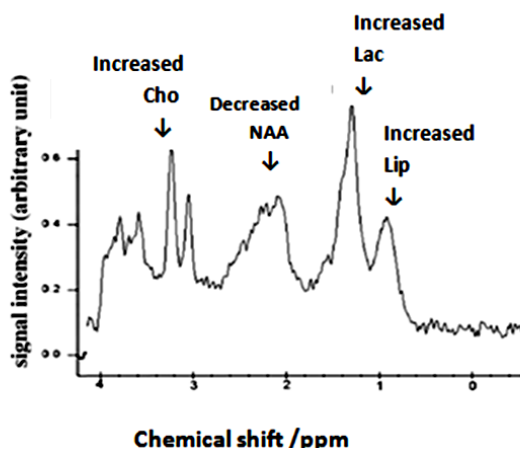


Figure C. MR spectroscopy of glioblastoma .The spectra represent the x-axis as chemical shift in ppm and the y-axis as signal intensity. The spectrum shows an increased peak of choline (Cho), a decreased peak of N-acetyl aspartate (NAA), and a decreased peak of creatine (Cr). The glioblastoma are characterised by a significant increase in lipid (Lip) and lactate (Lac).

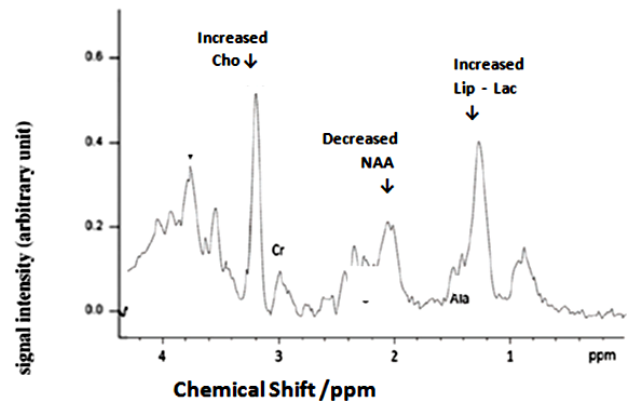


Figure B. MR Spectroscopy of Cerebellopontine Angle Tumor. The graph represents signal intensity versus chemical shift (ppm) in the y-axis and x-axis, with an elevated peak of choline (Cho) and a decreased peak of N-acetyl aspartate (NAA) and creatine (Cr). The increased peak of lipid (Lip) and lactate (Lac) gives the characteristic feature of a cerebellopontine angle tumor.

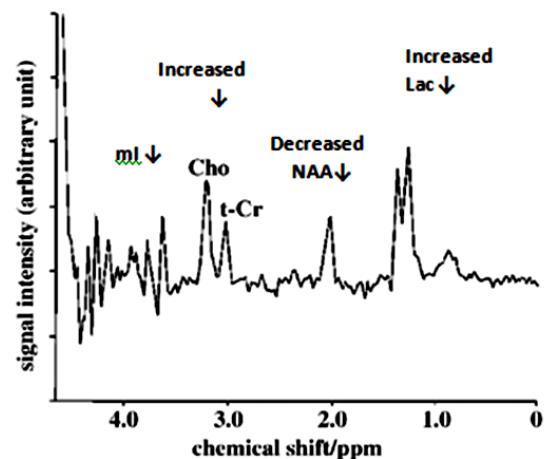


Figure D. MR spectroscopy of glioma .The spectrum demonstrates chemical shift (ppm) on the x-axis and signal intensity on the y-axis. The spectrum shows an elevated peak of choline (Cho), a diminished peak of N-acetyl Aspartate (NAA), and a low peak of creatine (Cr). The presence of lactate (Lac) and myoinositol (ml) indicates a characteristic feature of glioma.

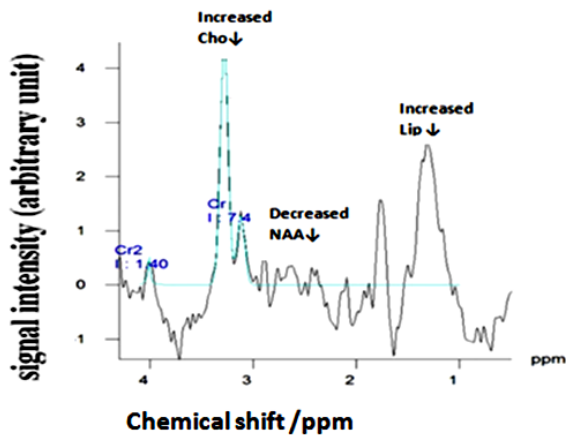


Figure E. MRS spectroscopy of lymphoma The x-axis represents the chemical shift in ppm, and the y-axis represents the signal intensity. The spectrum shows an elevated peak of lipid (Lip), which is an indicator of lymphoma. Other features like a decreased peak of N-Acetyl Aspartate (NAA) and an elevated peak of choline (Cho) are given.

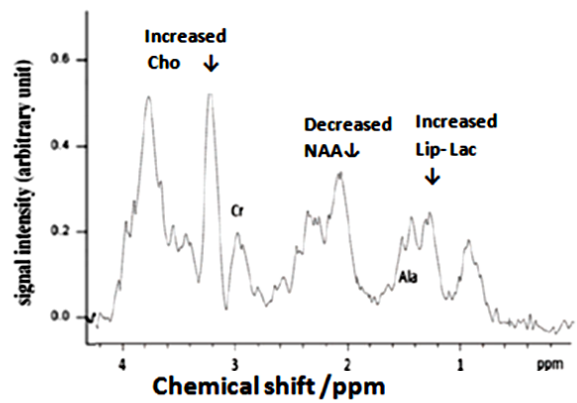


Figure F. MR spectroscopy of meningioma The x-axis is represented as chemical shift in ppm, and the y-axis is represented as signal intensity. The spectrum shows the presence of an elevated peak of choline (Cho), a decreased peak of N-Acetyl Aspartate, and creatine (Cr). The presence of alanine (Ala), lipid (Lip), and lactate (Lac) indicates the significant feature of meningioma.

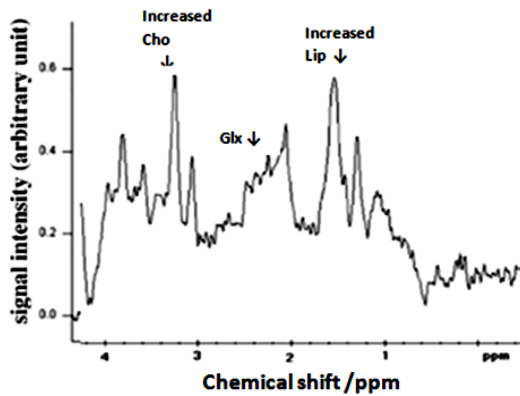


Figure G. MR spectroscopy of metastases The spectroscopy shows an elevated peak of choline (Cho), lipids (Lip), and glutamine and glutamate (Glx), which indicates the characteristic features of metastases.

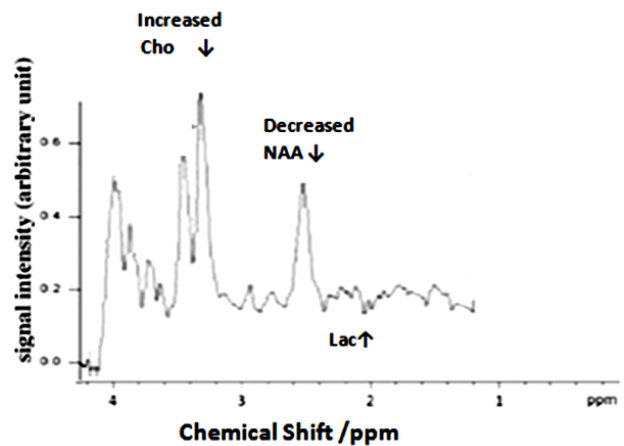


Figure H. MR spectroscopy of oligodendroglioma .The spectrum represents signal intensity on the y axis and chemical shift in ppm on the x-axis. The spectrum shows the presence of lactate (Lac), an increased peak of choline (Cho), and a diminished peak of N-acetyl aspartate (NAA), indicating the characteristic features of oligodendroglioma.

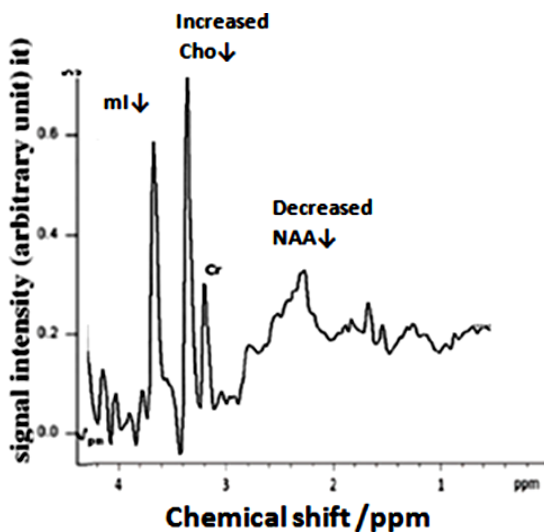


Figure I. MR spectroscopy of Subependymoma. The spectroscopy shows the signal intensity on the y-axis versus the chemical shift on the x-axis. The presence of myo-inositol (mi), an increased peak of choline (Cho), and a decreased peak of N-acetyl aspartate (NAA) and creatine (Cr) in the spectrum indicates the significant feature of subependymoma.

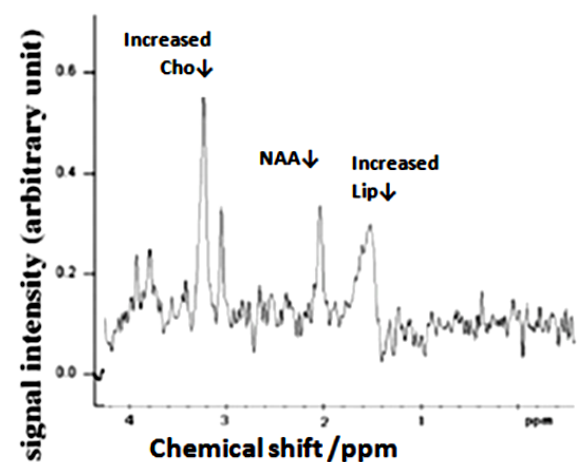


Figure J. MR spectroscopy of Tuberculoma .The spectrum represents the x and y axis as chemical shifts in ppm and signal intensity. It shows an increased peak of lipid (Lip) and choline (Cho) and a decreased peak of creatine (Cr) and N-Acetyl Aspartate (NAA) as an indicator of tuberculoma.

Table 1. Pathological finding of Brain tumors.

SL No	Brain tumors Lesions	Pathological description
1	Lymphoma	diffuse large B-cell lymphomas
2	Tuberculoma	Clusters of small nodules was observed in tuberculosis
3	Meningioma	Lobules, "meningothelial" whorls
4	Metastatis	demarcated, spherical masses and shiny mucoid appearance
5	Glioblastoma	hypercellularity, nuclear atypia, microvascular proliferation, and necrosi
6	Glioma	hypercellularity, nuclear atypia, mitotic figures, and evidence of angiogenesis and/or necrosis
7	Oligodendrogloma	round to oval, water-clear cytoplasm ringing about round to lobulated nuclei.
8	Cerebellopontine lesion	as encapsulated; biphasic, degenerative changes, nuclear pleomorphism, xanthomatous change and loose sheet of cells
9	Subependymoma	mitotic activity, microcalcifications, cystic degeneration, nuclear pleomorphism, vascular sclerosis, and hemosiderin deposition.
10	Adenoma	granulated GH-producing cells admixed with large atypical ganglion cells

Table 2. Comparison of MRS findings and Histopathologic findings.

Sl. No	Brain Tumors Lesions	MRS Specific metabolites	Histopathologically observed Metabolites	End products of metabolic pathway
1	Lymphoma	Lipid	Lipid	adipophilin
2	Tuberculoma	Lipid	Lipid	Triacylglyceride(TAG)
3	Meningioma	lipid	Lactate Lipid	Phosphoenolpyruvate carboxykinase Adipophilin, Phospholipid
4	Glioblastoma	Lipid Alanine	Lipid	glycosphingolipids
5	Glioma	Lactate Glycine	lactate	lactate dehydrogenase A (LDHA)
6	Oligodendrogloma	Lactate Lipid myo inositol	lipid	transforming growth factor β 2 (TGF β 2) triglycerides phospholipids sphingolipid prostaglandins
7	Cerebellopontine	myo inositol Glycine Glx (glutamate / glutamine)	myo inositol Glycine	protein C kinase
8	Subependymoma	Lipid	lipid	galactolipid cholesterol phospholipids
9	Adenoma	Lactate glycine myoinositol	Lactate	Lactate dehydrogenase
10	Metastatis	Lactate glutamine Lipid	lipid	adiponectin, leptin eicosanoids phosphoinositol sphingolipids

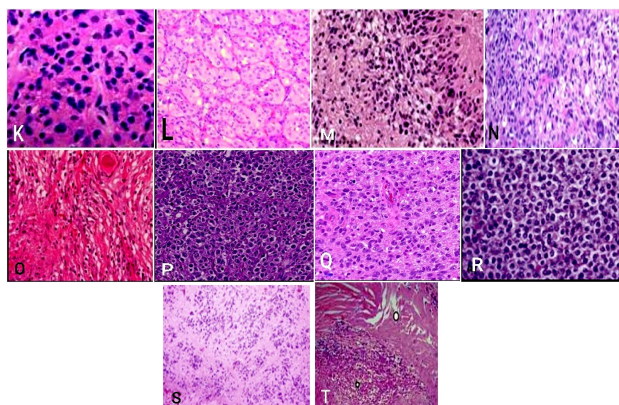


Figure K. Histopathological photomicrographs of brain tissues showing K Adenoma; L Cerebellopontine angle tumor; M Glioblastoma; N Glioma; O Meningioma; P Lymphoma; Q Metastatis; R Oligodendrogloma; S Subependymoma; T Tuberculoma

DISCUSSION

In the present study, the patients with different types of brain tumors were included and analyzed. Both histopathological and MRS findings were analysed. MRS has been used to determine the concentration levels of the intracellular metabolite and the metabolite compounds that serve as biomarkers. Similarly, pathological investigation helps us to study molecular pathways and interactions through the detection and monitoring of small molecular compounds. MRS imaging technique has been used to study the metabolite concentration levels. Histopathological studies were also included to find out pathological changes in brain tumors. In this study, 69 brain tumors with), adenoma (n=6), cerebellopontine angle tumor (n=9), glioblastoma

(n=6), glioma (n=4), lymphoma (n=6), meningioma (n=19), metastasis (n=8), oligodendroglioma (n=4), subependymoma (n=4) and tuberculoma (n=3) were analyzed. In the present study, the MRS spectrum of adenoma shows lipids, and the pathological studies demonstrated that the adenoma appeared as granulated GH-producing cells admixed with large atypical ganglion cells. Sarah *et al.* ⁽¹⁸⁾ detected that in adenomas, through the pathological analysis, there are characteristics of granular cytoplasm, which are also detected in our findings. Previous studies also indicated that pituitary adenoma alters the transcription of lipid-metabolism-related genes and the secretion of IL-6, adiponectin, and leptin ⁽¹⁹⁾.

In this study, it was detected that in the case of cerebellopontine angle tumors, the spectra were given as lipid and lactate peaks. Present studies also recognized that pathologically it appeared as encapsulated; biphasic, degenerative changes, nuclear pleomorphism, xanthomatous change, and a loose sheet of cells. Previous studies also showed that the pathology of cerebellopontine lesions was presented as loose sheets of cells with pleomorphic changes ⁽²⁰⁾. The findings of the MRS spectrum of glioblastoma (GBM) in the present study indicate that there is an increase in lipids, lactate, and glycine concentrations. These results confirm the existing evidence in the studies of glioblastoma with an increased level of choline and lipids, as observed by MRS ⁽²¹⁾.

In another study, it was mentioned that the level of glycine peak is significantly higher for the diagnosis and prognosis of glioblastoma, which is diagnosed through MRS ⁽²²⁾. Pathologically, the present study in glioblastoma shows the features of hypercellularity, nuclear atypia, microvascular proliferation, and necrosis. Glioblastoma with high proliferative potential is also an infiltrative brain tumor, according to research. Studies also showed that glioblastoma with high proliferative potential infiltrate brain tumor ⁽²³⁾. An interpretation of the findings reveals a connection between lipids and glycosphingolipids. According to the studies it was found that in GBM the pyruvate can be converted to lactate and also the GBM synthesizes lipids and lipid signaling molecules needed to proliferate ⁽²⁴⁾.

Previous studies also enumerated that in GBM, lipid metabolism results in the conversion of glycosphingolipids ⁽²⁵⁾. This study also provides new insights into the connection between lactate and lactate dehydrogenase A in GBM patients. Arunpreet *et al.* ⁽²⁶⁾ confirmed that lactate production is increased in GBM patients, as well as overexpression of LDHA (lactate dehydrogenase A). Present studies determined that the MRS spectrum of glioma gives a lactate peak and an increased level of myoinositol. In one of the studies also it was reported, an increased level of myoinositol in glioma ⁽²²⁾. Pathologically the present study determined that

glioma shows hypercellularity, nuclear atypical, and mitotic figures. Candece *et al.* ⁽²⁷⁾ also showed that grade II glioma tumors are graded according to the presence of hypercellularity. In the study by Strickland *et al.* ⁽²⁸⁾ it was found that glioma metabolizes glucose and the end product is lactate which is released into the extracellular space. Baumann *et al.* ⁽²⁹⁾ also revealed that lactate induces the expression of transforming growth factor $\beta 2$ (TGF $\beta 2$).

In addition to that studies also realized that an increased rate of lipids, including mobile fatty acids, triglycerides, phospholipids, cholesterol esters, sphingolipids, prostaglandins, and steroid hormones acts as a cellular membrane breakdown ⁽³⁰⁾. In this study, the spectrum of oligodendroglioma gives an increased level of myoinositol, glutamate/glutamine (GLX). In the current investigation, it was discovered that lymphoma has an elevated lipid peak in the MRS spectrum. However, studies also found that elevated lipid peaks were seen in tumors such as lymphomas ⁽³¹⁾. Similarly, the current histopathological results demonstrate the presence of large diffuse B-cell lymphomas. Studies have revealed that lymphoma is a tumor of immature B cells and that these cells' receptors affect how antibodies work ⁽³²⁾. The investigations also recognized the potential of adipophilin, a protein found in lipid storage droplets (LSDs), as a Burkitt lymphoma marker ^(33, 34).

The present study shows that the MRS spectrum of meningioma gives increased lactate and lipid peaks. Alanine and glutamate were also shown as high concentrations. In the previous studies, it was evident that alanine is present in meningioma, diagnosed through MRS ⁽³⁵⁾. The present study reveals that meningioma also gives a pathological appearance as lobules, "meningothelial" whorls. Meningothelial cells in meningiomas have been described as forming spherically in earlier research, associated with a greater lipid concentration, which is also seen in the current study. Adipophilin is employed as an immunohistochemical marker that is linked to lipid droplets, according to investigations that have been done previously ⁽³⁶⁾. In this study, it was observed that in the MRS spectrum of metastases, metabolites like lipids, and glutamine/glutamate complex were increased. This result showed that metastasis, as previously shown by MRS analysis in studies, had a higher level of lipid ⁽³²⁾. In the present histopathological study, it was revealed that metastasis appeared as demarcated, spherical masses and shiny mucoid appearance. Earlier studies show that metastatic lesions are usually sharply demarcated according to the histopathological study ⁽³⁷⁾.

Another study also revealed that in metastasis, most of the lactate is seen outside the cells. Apart from this, studies also revealed that due to the avidity of lipid metabolism, the signaling lipids like

eicosanoids, phosphoinositides, sphingolipids, and fatty acids, might be the causal factor of tumor malignant and metastasis⁽³⁸⁾. The current findings give more understanding of the tumor oligodendroglioma as the previous studies also reported that there is an increased level of GLX in oligodendroglioma when compared to other tumors⁽²²⁾. The presence of microvascular proliferation, water-clear cytoplasm ringing around the round to lobulated nuclei, and necrosis, according to this study, can improve the pathological diagnosis of tumor oligodendroglioma. Previous studies also confirmed that oligodendroglioma shows the appearance of mitotic activity, microvascular proliferation, and necrosis⁽³⁹⁾.

Earlier studies indicate that oligodendroglioma has higher levels of myoinositol and acts as an activator of protein C kinase⁽⁴⁰⁾. In the case of subependymoma, the present studies determined that MRS of subependymoma gives myoinositol (MI) and glycine (Gly) peaks. Pathologically in this study, it was found that the subependymoma appeared with mitotic activity, microcalcifications, cystic degeneration, nuclear pleomorphism, vascular sclerosis, and hemosiderin deposition. Studies have found that subependymoma shows histologically that it appeared as numerous small cysts⁽⁴¹⁾. In addition to that, previous studies also confirmed that in cancer cells, an increased level of lactate dehydrogenase A (LDHA) leads to the enhancement of the malignant phenotype⁽⁴²⁾. In this study, it was found that the MRS of tuberculoma contains abnormally high levels of lipids and glutamate. It was confirmed in one of the earlier investigations that tuberculoma can be diagnosed with an elevated amount of lipid and amino acids using MRS⁽⁴³⁾. According to histopathology, there were groups of tiny nodules. Previous research also suggested that abscess and fibrous encapsulation could develop as a result of tuberculoma lesions⁽⁴⁴⁾.

Studies have also shown that TAG (triacylglyceride) is the storage lipid present in tuberculous granulomas and that lactate is formed following infection. The single discovered gene, transcript, and protein was pckA (phosphoenolpyruvate carboxykinase)⁽⁴⁵⁾. The limitations of this study are the limited data collection. In this study, MRS analysis information of tumors associated with underlying pathophysiological findings provides the best diagnostic clue for further tumor treatment as early as possible.

CONCLUSIONS

Magnetic Resonance Spectroscopy and the pathological findings provide the quantification of tissue metabolite concentration, which helps to assess the impact on the clinical outcome as specific

markers. Thus MRS can potentially identify the pathological change, at the biochemical level which helps in further therapeutic interventions.

ACKNOWLEDGEMENT

The authors express their appreciation and gratitude to Dr. Manju. L, Associate Professor, Department of Community Medicine, Sree Gokulam Medical College and Research Foundation for her kind support in this study for statistical evaluation and interpretation.

Conflict of interest: All authors declared that they have no conflict of interest.

Ethical considerations: The study followed the rules of the ethics committee for using the patients for scientific purposes after obtaining approval from the SGMC Institutional Ethics Committee (IEC) (registration number: SGMC-IEC NO 31/383/11/2018 (F) and date of registration: 26:11:2018).

Funding: This research did not receive any specific grant from funding agencies in the public, commercial, or not-for-profit sectors.

Author Contributions: S.H, the first author of the article is the principal investigator of the study. She did the data collection, analysis and preparation, and typing of the manuscript. The second author, M.D.V.N. was involved in coordinating the work and giving valuable suggestions for modifications. S.K.S, the third author of the article contributed to the preparation of the manuscript, corrections, data interpretation for analysis, and interpretation of change in metabolites in MRS. V.J., the fourth author provided the patients for the study and helped in the interpretation of the report of MRS.

REFERENCES

1. Aldape K, Brindle KM, Chesler L, et al. (2019) Challenges to curing primary brain tumors. *Nature Reviews, Clinical oncology*, **16**(8): 509-520.
2. Qi X, Jha SK, Jha NK, et al. (2022) Antioxidants in brain tumors: current therapeutic significance and future prospects. *Mol Cancer*, **21**(204): 1-32.
3. G Elshaikh BG, Omer H, Garelnabi MEM, et al. (2021) Incidence, diagnosis and treatment of brain tumours Buthayna. *Journal of Research in Medical and Dental Science*, **9**(6): 340-347.
4. Cooper GM (2000) The Cell: A Molecular Approach. *Sinauer Associates, Sunderland, Massachusetts*.
5. Mohammed AA, Hamdan AN, Homoud AS (2019) Histopathological profile of brain tumors a 12-year retrospective study from Madinah, Saudi Arabia. *Asian J Neurosurg*, **14**(4): 1106-1111.
6. Bukhtoyarov O and Samarin D (2015) Pathogenesis of cancer: Cancer reparative trap. *Journal of Cancer Therapy*, **6**: 399-412.
7. Pichaveil M, Anbumani G, Theivendren P, Gopal M (2022) An overview of brain tumor. *Brain tumors. Intechopen*, **1**(1): 1-212.
8. De Berardinis RJ and Chandel NS (2016) Fundamentals of cancer metabolism. *Sci Adv*, **2**(5): 1-65.
9. Shetty JK, Prasad KHL, Shruthi S (2022) Raghorthaman a, challenges in the histopathologic diagnosis of brain tumors: An institutional experience in a series of cases. *Journal of Health and Allied Sciences*, **12**(4): 412-416.
10. Perkins A and Liu G (2016) Primary brain tumors in adults: Diagnosis and treatment. *American Family Physician*, **93**(3): 1-9.

11. Weinberg BD, Kuruva M, Shim H, Mullins ME (2021) Clinical applications of magnetic resonance spectroscopy in brain tumors: From diagnosis to treatment. *Radiologic clinics of North America*, **59**(3): 349–362.
12. Franco P, Würtemberger U, Dacca K, et al. (2020) Spectroscopic prediction of brain tumors (SPORT): study protocol of a prospective imaging trial. *BMC Med Imaging*, **20**(123): 1-7.
13. Tognarelli JM, Dawood M, Shariff MI, et al. (2015) Magnetic resonance spectroscopy: Principles and techniques: Lessons for clinicians. *J Clin Exp Hepatol*, **5**(4): 320-328.
14. Onyambu CK, Wajih MN, Odhiambo AO (2021) Clinical application of magnetic resonance spectroscopy in diagnosis of intracranial mass lesions. *Radiology Research and Practice*, **2021**(1):1-10.
15. Gujar SK, Maheshwari S, Björkman-Burtscher I, Sundgren PC (2005) Magnetic Resonance Spectroscopy. *J Neuroophthalmol*, **25**(3): 217-26.
16. Ciurleo R, Di Lorenzo G, Bramanti P, Marino S (2014) Magnetic resonance spectroscopy: An in vivo molecular imaging biomarker for parkinson's disease? *BioMed Research International*, **2014**(1): 1-10.
17. Marie SKN and Shinjo SMO (2011) Metabolism and brain cancer. *Clinics*, **66**(S1): 33-43.
18. Sarah L and Olaf A (2017) Pathology and pathogenesis of pituitary adenomas and other sellar lesions. *Endotext (internet)*, 1-45.
19. Zheng X, Li S, Zhang WH, Yang H (2015) Metabolic abnormalities in pituitary adenoma patients: a novel therapeutic target and prognostic factor. *Diabetes Metab Syndr Obes*, **8**: 357-361.
20. Karki KT and Koirala SJ (2017) An unusual variant of cerebellopontine angle schwannoma in a young Nepalese girl journal of clinical & experimental pathology. *Clin Exp Pathol*, **7**(2): c307.
21. xMcManaman JL, Zabaronick W, Schaack J, Orlicky DJ (2003) Lipid droplet targeting domains of adipophilin. *Journal of Lipid Research*, **44**(4): 668-673.
22. Ashish V, Ishan K, Nimisha V, et al. (2016) Magnetic resonance spectroscopy Revisiting the biochemical and molecular milieu of brain tumors. *BBA Clinical*, **5**: 170-178.
23. Akira H, Tomohiro K, Kei N, et al. (2019) Treatment strategies based on histological targets against invasive and resistant glioblastoma. *Journal of Oncology*, **2019**: 1-10.
24. Zhou W and Wahl D (2019). Metabolic abnormalities in glioblastoma and metabolic strategies to overcome treatment resistance. *Cancers*, **11**(1231): 1-26.
25. Catherine JL, Anh NT, Sarah ES, (2019) The pro-tumorigenic effects of metabolic alterations in glioblastoma including brain tumor initiating cells. *BiochimBiophysActa Rev Cancer*, **1869**(2): 175-188.
26. Arunpreet SK, Mariam A, Arundeeep K, Jonathan W (2016) Lactate levels with glioblastoma multiforme. *Proceedings (Baylor University Medical Center)*, **29**(3): 313-314.
27. Candece LG, Richard AP, Wei M, LiuAR (2010)The Pathobiology of Glioma Tumors. *Pathol*, **5**: 33-50.
28. Strickland M and Stoll EA (2017) Metabolic reprogramming in glioma, a stoll, *frontiers in cell and development. BiologyFront. Cell Dev Biol*, **5**(43): 1-32.
29. Baumann F, Leukel P, Doerfelt A, et al. (2009) Lactate promotes glioma migration by TGF-beta2-dependent regulation of matrix metalloproteinase-2. *Neuro Onco*, **11**(4): 368-80.
30. Pohchoo S, Vairavan N, Aditya TH, et al. (2018) Quantification and visualization of lipid landscape in glioma using in -and opposed-phase imaging. *NeuroimageClinical*, **20**: 531-536.
31. Grabovetskyi S (2015) Proton magnetic resonance spectroscopy of focal intracranial lesions: Role in clinical practice, *J Cancer PrevCurr Res*, **2**(5): 1-16.
32. Malcolm TIM, Hodson DJ, Macintyre EA, Turner SD (2016) Challenging perspectives on the cellular origins of lymphoma. *Open Biol*, **6**(9): 1-12.
33. Ambrosio MR, Piccaluga PP, Ponzoni M, et al. (2012) The alteration of lipid metabolism in Burkitt lymphoma identifies a novel marker: Adipophilin. *PLoS one*, **7**(8): 1-7.
34. McManaman JL, Zabaronick W, Schaack J, Orlicky DJ (2003) Lipid droplet targeting domains of adipophilin. *Journal of Lipid Research*, **44**(4): 668-673.
35. Alena H and Peter BB (2010) Imaging of Brain Tumors: MR spectroscopy and metabolic imaging neuroimaging. *Clin N Am*, **20**(3): 293-310.
36. Ishida M, Fukami T, Nitta N, et al. (2013) Case report xanthomatous meningioma: a case report with review of the literature. *Int J Clin Exp Pathol*, **6**(10): 2242-224.
37. Melike P and Arie P (2013) Neuropathology of brain metastasis. *Surgical Neurological International*, **4**(4): S245-55.
38. Xiangjian L, Xu Z, Can C, et al. (2018) The implications of signaling lipids in cancer metastasis. *Experimental & Molecular Medicine*, **50**(9): 1-10.
39. Pieter W, Martin van den B, Arie P (2015) Oligodendroglioma: pathology, molecular mechanisms, and markers. *ActaNeuropathologica*, **129**(6): 809-827.
40. Lina MA, Tommy BA, Soma G, et al. (2015) Metabolomic Screening of Tumor Tissue and Serum in Glioma Patients Reveals Diagnostic and Prognostic Information. *Metabolites*, **5**: 502-520.
41. Koeller KK and Sandberg GD (2002) Cerebral intraventricular neoplasms: Radiologic-pathologic correlation. *Radiographics*, **22**(6): 1473-505.
42. Marie SK and Shinjo SM (2011) Metabolism and brain cancer. *Clinics (Sao Paulo)*, **66**(1): 33-43.
43. Oz G, Alger JR, Barker PB, et al. (2014) Clinical proton MR spectroscopy in central nervous system disorders. *Radiology*, **270**(3): 658-79.
44. John MLA (2014) Chapter 41 - Tuberculosis of the Central Nervous System Neurology and General Medicine: Fifth Edition
45. Sandra B, Marie S, Claudia H, et al. (2017) Lactate oxidation facilitates the growth of Mycobacterium tuberculosis in human macrophages. *Scientific Reports*, **7**(6484): 1-12.

